Partially converged integral equations for charged colloidal suspensions with added salt

2005 J. Phys.: Condens. Matter 17 7935

(http://iopscience.iop.org/0953-8984/17/50/012)

INSTITUTE OF PHYSICS PUBLISHING JOURNAL OF PHYSICS: CONDENSED MATTER

J. Phys.: Condens. Matter **17** (2005) 7935–7953 doi:10.1088/0953-8984/17/50/012

Partially converged integral equations for charged colloidal suspensions with added salt

Juan A Anta

Departamento de Ciencias Ambientales, Universidad Pablo de Olavide, Carretera de Utrera, Km 1, 41013 Sevilla, Spain

Received 17 January 2005, in final form 2 September 2005
Published 2 December 2005
Online at stacks.iop.org/JPhysCM/17/7935

Abstract

We explore the possibility of using a simplified version of the multicomponent hypernetted-chain (HNC) integral equation for charged colloidal suspensions. The method presented here is an extension of a previous one (Anta *et al* 2003 *J. Phys.: Condens. Matter* **15** S3491) for systems with added salt. Within this theoretical scheme, colloid–colloid, colloid–microion and microion–microion correlations are treated with different levels of approximation. Thus, we describe microion–microion correlations in the random phase approximation (RPA) whereas colloid–microion and colloid–colloid correlations are solved in the HNC approximation. This strategy reduces the numerical demands of the full HNC equation and makes it possible to get a solution at thermodynamic states not included in the original solution region. In addition, it is found that we can extend even further the range of applicability of the theory by solving the colloid–microion part of the theory for a fixed colloid–colloid radial distribution function. This is obtained in turn from the solution of the one-component HNC equation for the effective DLVO potential. Using these strategies we obtain a semi-quantitative description of the colloidal system as well as an indication of a salt-driven phase transition at low ionic strengths. This phase transition is associated to charge inversion, as inspection of the colloid–microion density profiles reveals. However, the theory fails to reproduce reliable effective-pair potentials in the vicinity of the non-solution region. The applicability and usefulness of integral equation theories when applied to charged colloids is discussed.

(Some figures in this article are in colour only in the electronic version)

1. Introduction

Colloidal suspensions are multi-component systems characterized by large asymmetries in size and charge [1, 2]. They possess a very rich phase behaviour and exhibit a variety of structures and microscopic orderings which, in many cases, are analogous to those observed in molecular systems [3]. This analogy has encouraged theorists to extend methods which are successful

in the description of simple and molecular fluids to the explanation of a number of colloidal phenomena.

Due to this asymmetry in size and charge characteristic of a colloidal system, the simplest way of formulating a theoretical description of its structure and interactions is by *coarse-graining*. By coarse-graining we mean to eliminate the degrees of freedom of the smaller and less charged particles so that the mixture is treated as an effective one-component system (OCS) of large particles. The well-known Derjaguin–Landau–Verwey–Overbeek (DLVO) theory and effective potential [4], widely used nowadays in colloidal science, is nothing else but a particularly successful example of a coarse-graining procedure. The DLVO effective potential was obtained originally from the linearized Poisson–Boltzmann (PB) equation but it can also be derived in the context of density functional theory (DFT) [5, 6] and linear response theory [7, 8]. All these approaches are based on a simplified description of the colloid–microion correlation and the structure of the 'ionic atmosphere' around a spherical colloid. They make it possible to formulate an approximate free energy functional from which an effective interaction is extracted by integrating out the degrees of freedom of the ions. Together with the correct derivation of the DLVO effective pair potential, these theories show the importance of one-body terms in the free energy expansion. For instance, these one-body terms are found to contribute to the thermodynamic behaviour of the system and predict phase separation at low ionic strengths [5].

Linearized PB, mean-field DFT and LRT have the following common features.

(1) They treat microion–microion correlations in the simplest approximation (mean-field or random phase approximation).
(2) Colloid–microion correlations are solved at a *linearized* level, that is, they ignore higher-order terms in a certain free energy expansion.
(3) Colloid–colloid correlations are not considered.

Extensions over these linearized approaches have also been explored [8–10]. In general, these extensions are reduced to improve on point (2) above. Thus, it has been seen that linear PB theory leads to a spurious phase separation which is not found in the full solution of the PB equation [9]. Also, the introduction of non-linear terms in the free energy functional implies that the effective potential is no longer pairwise additive [8]. As regards points (1) and (3), some improvements have been accomplished recently. Microion–microion correlations can be implicitly considered via an effective potential [11]. PB theory can also be solved at 'finite colloidal density' to obtain effective colloidal charges [12]. In summary, the partial success of these linearized theories demonstrates that it might not be necessary to include a full description of all correlations to obtain useful results. We will make use of this fact below.

As an alternative to the aforementioned theories, simulation techniques provide an 'exact' description of all correlations involved in the colloidal mixture [13–18]. Simulations of charged colloidal systems have shown that many phenomena occurring in these systems such as like-charge *effective* attraction [16], overcharging [15], phase behaviour departing from simple DLVO theory [14], and reentrant transitions [17], arise from many-body electrostatic interactions only. However, direct application of simulation techniques is cumbersome due to the strong asymmetry characteristic of these systems. This numerical limitation has hindered an adequate consideration of the influence of colloid–colloid correlations and the effect of added electrolyte, especially in the regimes of low ionic strength and high colloidal charges. Still, simulations remain as the method of reference to test the accuracy of other theories.

Another group of methods coming from the field of classical fluids are integral equation theories [19]. These theories, when applied to colloidal systems [20, 21], have the following advantages.

(1) They include colloid–colloid, colloid–microion and microion–microion correlations explicitly and more precisely than 'simple' approaches (PB, DFT, etc).
(2) They are numerically less demanding than simulations.
(3) They allow for an unambiguous definition of a *pairwise additive* effective potential between colloids. In other words, they provide a convenient way of doing *coarse-graining* [22].

On the other hand, they suffer from the following drawbacks.

(1) They are algebraically very complex.
(2) They exhibit a frustrating *non-solution* region which does not necessarily coincide with regimes of physical instability [23, 24].

In this paper we explore the capability of integral equation theories to provide useful results in colloidal systems in spite of these drawbacks. With this intention we have proposed in previous papers [25, 26] a simplified integral equation based on the solution of the multi-component Ornstein–Zernike equation [3] coupled with three different closures. In this approach the complexity and accuracy of the closure used depends on the correlation to be described. Thus microion–microion correlations are treated in the simplest random phase approximation (RPA). In turn, the colloid–microion correlations are obtained from the solution of the hypernetted-chain (HNC) equation for a charged spherical colloid surrounded by counterions. Finally, the effective one-component system (OCS) is described by the HNC or the reference-HNC (RHNC) approximation. Since the definition of the OCS, via an effective pair potential, depends on the colloid–microion structure, the whole procedure should be iterated until self-consistency. This strategy, which we call 'coarse-grained' HNC theory (CGHNC), proves to be accurate enough to reproduce exact colloid–colloid and colloid–ion correlation functions in salt-free colloidal suspensions [25]. In addition, it broadens the solution region of the integral equation without losing significant accuracy in the description of the effective one-component system and the 'ionic' atmosphere around the spherical colloid [26].

The aim of this paper is twofold. First we present an extension of the CGHNC theory to the case of added electrolyte and test its performance against simulation and experimental results. Second we discuss the capability of integral equation theories to provide useful results in charged colloidal suspensions. In this regard we will see that, although the CGHNC reduces the numerical and algebraic complexity of the multi-component Ornstein–Zernike equation, this integral equation remains unsolvable for a large number of cases. This serious shortcoming places us against the dilemma of disregarding these kinds of theory because they do not provide a solution for *all* cases in spite of the fact that they give *quick* and accurate results in the *rest* of the cases. In order to make progress on this issue, we discuss the nature of the non-solution line in charged-colloidal suspensions by looking at the effective potential in the proximity of the non-solution boundary. Furthermore we explore the alternative of obtaining colloid–microion radial distribution functions and colloid–colloid effective potentials without requiring a full self-consistent solution of the integral equation.

The outline of the paper is as follows. In section 2 we briefly present the derivation of the CGHNC theory for suspensions with added salt and the numerical strategy used to implement it. In section 3 we test the performance of the theory by comparing with simulations and experimental data. In section 4 we make use of the theory to provide an explanation of a 'reentrant' phase transition recently reported in the literature. The origin of the non-solution region of the integral equation and the efficiency of our formalism is discussed in section 5. Finally, in section 6, the main conclusions of this work are summarized.

2. The CGHNC theory

In the present work we consider a system of ionized colloidal particles with positive charge z_c in the presence of their corresponding negatively charged counterions of charge z_i. The number density of the colloids is ρ_c, whereas the density of the counterions is given by the charge electroneutrality condition; hence $\rho_i = (z_c/z_i)\rho_c$. In addition we consider a salt electrolyte of concentration ρ_s which contributes to the system with cations of charge z_+ and anions of charge z_-. The electroneutrality condition also requires that $z_+\rho_+ = z_-\rho_-$, where ρ_+ and ρ_- are, respectively, the density of cations and anions coming from the added electrolyte. Our mixture is, therefore, a four-component system. In the following, we will refer to both the counterions and salt ions as 'microions'.

All species in the system interact via pair potentials of the type

$$u_{mn}(r) = u_{mn}^{\mathrm{SR}}(r) + \frac{z_m z_n e^2}{4\pi\varepsilon r}, \qquad (m, n = c, i, +, -) \tag{1}$$

where u^{SR} is a short-range interaction[1] (for instance, a hard-core repulsion term) and ε is the permittivity of the solvent, which is taken as a continuum.

The colloidal system so defined poses a formidable problem. We have to solve for ten different correlations, involving microions with microions, colloid with microions and colloids with colloids. In the following we will see how we can take advantage of the asymmetry of the mixture to reduce the complexity of the problem and facilitate its numerical solution. In order to do this we proceed as follows.

Step 1: many-body problem

In the integral equation formalism, many-body interactions are treated by means of the Ornstein–Zernike (OZ) equations [3]. For a multicomponent mixture they can be written as

$$h_{mn}(r) = c_{mn}(r) + \sum_{l=1}^{M} \rho_l \int \mathrm{d}\mathbf{r}_l \, c_{ml}(r) h_{ln}(r) \tag{2}$$

where M is the total number of components in the mixture and $h_{mn}(r)$ and $c_{mn}(r)$ are, respectively, the total correlation function (TCF) and direct correlation function (DCF) between species m and n. The total correlation functions are related to the Ashcroft–Langreth partial structure factors $S_{mn}(k)$s via [27]

$$S_{mn}(k) = \delta_{mn} + (\rho_m\rho_n)^{1/2} \int_V \mathrm{d}\mathbf{r}\, \mathrm{e}^{\mathrm{i}\mathbf{k}\cdot\mathbf{r}} h_{mn}(r) = \delta_{mn} + (\rho_m\rho_n)^{1/2} h_{mn}(k), \tag{3}$$

with the $h_{mn}(k)$s being the Fourier transforms of the total correlation functions (TCFs).

The OZ equations are exact relations between *all* TCFs, which describe the pair structure of the system. They can be regarded as the definition of the DCFs. It can be also shown that the DCFs are related to the second-order functional derivatives of the excess free energy of the system [3, 28, 29].

Taking the Fourier transform of equation (2) and using matrix notation we obtain

$$\mathbf{H}(k) = \mathbf{C}(k) + \mathbf{C}(k) \cdot \mathbf{H}(k) \tag{4}$$

where $\mathbf{H}$ and $\mathbf{C}$ are $M \times M$ matrices whose elements are defined by

$$\begin{aligned} [\mathbf{H}(k)]_{mn} &= (\rho_m\rho_n)^{1/2} h_{mn}(k); \\ [\mathbf{C}(k)]_{mn} &= (\rho_m\rho_n)^{1/2} c_{mn}(k). \end{aligned} \tag{5}$$

[1] In this paper we have considered hard-core interactions only. Nonetheless the theory and its corresponding numerical program are also straightforwardly applicable to soft interactions.

Combining equations (3) and (4) we can express the OZ equations as a matrix relationship between partial structure factors and DCFs

$$\mathbf{S}(k) = [\mathbf{I} - \mathbf{C}(k)]^{-1} \tag{6}$$

where $\mathbf{I}$ is the identity matrix. In a one-component fluid, the OZ equations (6) reduce to the familiar form

$$S(k) = 1 - \rho h(k) = \frac{1}{1 - \rho c(k)}. \tag{7}$$

Step 2: coarse-graining

A central point in this formalism is to reduce the problem to an effective one-component system (OCS). To do this we take [22, 28]

$$S(k) = S_{\mathrm{cc}}(k) \tag{8}$$

where $S(k)$ is the structure factor of the OCS. Thus, the OCS is defined as the fluid whose characteristic pair structure is identical to the colloid–colloid pair structure of the original four-component system. Bearing in mind the OCS result (7) and

$$S_{\mathrm{cc}}(k) = \frac{\mathrm{cofactor}[1 - \rho_{\mathrm{c}} c_{\mathrm{cc}}(k)]}{\mathrm{Det}[\mathbf{I} - \mathbf{C}(k)]} \tag{9}$$

we find the following relationship between the DCF of the one-component system and the DCFs of the mixture

$$c(k) = c_{\mathrm{cc}}(k) - \frac{R^s(k)/\rho_s}{\mathrm{cofactor}[1 - \rho_{\mathrm{c}} c_{\mathrm{cc}}(k)]} \tag{10}$$

where $R^s(k)$ is the result of multiplying the second, third and fourth elements of the first row of matrix $\mathbf{I} - \mathbf{C}(k)$ by their respective cofactors and summing up the results. For the simpler case of a colloid–counterion mixture (no added salt) it can be shown that this expression reduces to [25]

$$c(k) = c_{\mathrm{cc}}(k) + \frac{\rho_{\mathrm{i}}[c_{\mathrm{ci}}(k)]^2}{1 - \rho_{\mathrm{i}} c_{\mathrm{ii}}(k)}. \tag{11}$$

Step 3: effective potential

According to Henderson's theorem [30], there is a unique pair potential that fully determines the pair correlation function of a fluid. Therefore, the OCS defined by equation (8) should lead to the definition of an effective *pair* potential between colloids. By using this strategy we make sure that the effective potential so constructed is *pairwise* by definition.

In order to find this we identify the pair distribution functions $g(r) = h(r) + 1$ of the OCS and the original mixture as well as their corresponding potentials of mean-force $w(r)$

$$g(r) = \exp[-\beta w(r)] = g_{\mathrm{cc}}(r) = \exp[-\beta w_{\mathrm{cc}}(r)] \tag{12}$$

where $\beta = 1/k_{\mathrm{B}}T$. The potential of mean-force can be related in turn to the DCFs, hence

$$-\beta u^{\mathrm{eff}}(r) + h(r) - C(r) - B(r) = -\beta u_{\mathrm{cc}}(r) + h_{\mathrm{cc}}(r) - C_{\mathrm{cc}}(r) - B_{\mathrm{cc}}(r) \tag{13}$$

where $u^{\mathrm{eff}}(r)$ is the effective potential and the B_{mn}s are the so-called *bridge functions*. The bridge functions are related to the 'higher-than-two' functional derivatives of the excess free energy functional with respect to the density profiles. Neglecting their contribution leads to the well-known HNC approximation. Otherwise, by including them in equation (13), we start

from an approach that is formally exact. We next use equation (10) to arrive at the following expression for the effective colloid–colloid pair potential

$$\beta u_{\rm eff}(r) = \beta u_{\rm cc}(r) + {\rm FFT}^{-1}\left[\frac{R^s(k)/\rho_{\rm c}}{{\rm cofactor}[1-\rho_{\rm c}{\rm c}_{\rm cc}({\rm k})]}\right] + [B_{\rm cc}(r) - B(r)]$$
$$= \beta u'_{\rm eff}(r) + [B_{\rm cc}(r) - B(r)] \tag{14}$$

where FFT^{-1} stands for inverse Fourier transformation.

Equation (14) shows that the effective interaction $u_{\rm eff}(r)$ between colloidal particles is a sum of three contributions: (1) direct colloid–colloid interaction, (2) microion-mediated interaction which depends on the colloid–microion and microion–microion DCFs and (3) a term that arises from the difference between the bridge function of the OCS and the colloid–colloid bridge function of the mixture. A convenient but somehow uncontrolled approximation is to assume that both bridge functions are essentially the same. We have seen elsewhere [26] that this is not necessarily true, especially in the vicinity of a non-solution boundary. Alternatively, we can assume that both bridge functions are zero, which is equivalent to treating all correlations in the HNC approximation. In any case, the simplest choice is to ignore this contribution. Thus, we can take $u_{\rm eff} = u'_{\rm eff}$ in equation (14) and the effective potential between colloids can be computed in terms of all the DCFs of the mixture only. We will see that this simplification works reasonably well in some cases although it may lead to 'unphysical' effective potentials which are responsible for non-solution instabilities.

Step 4: microion–microion correlations

The expression introduced above for the effective potential depends on the microion–microion correlations via the DCFs. We make use of the random phase approximation (RPA) to compute these. Hence

$$C_{mn}(r) = -\beta u_{mn}(r) \qquad (m, n = i, +, -). \tag{15}$$

With this approximation, we make the microion–microion correlations *independent* or *uncoupled* from the rest of the correlations in the mixture. In other words, we assume that colloids move in a sea of microions whose characteristic direct correlation functions behave as if the colloids were absent. This is an analogous approximation to the *jellium* approximation employed in liquid metals [28]. We have previously [25, 26] demonstrated that this simplification reduces the numerical complexity of the integral equation without significantly reducing its accuracy, at least for monovalent counterions.

A short-range term can be included, in principle, in equation (15). Nevertheless, we have observed that for very asymmetric systems this term does not significantly improve the results for the colloid–colloid and colloid–microion correlation functions.

Step 5: colloid–microion correlations

We treat this interaction in the HNC approximation. This means that the colloid–microion mean-force potential is obtained through

$$w_{\rm cm}(r) = \beta u_{\rm cm}(r) - h_{\rm cm}(r) + C_{\rm cm}(r) \qquad (m = i, +, -) \tag{16}$$

with

$$g_{\rm cm}(r) = h_{\rm cm}(r) + 1 = \exp[-\beta w_{\rm cm}(r)] \qquad (m = i, +, -). \tag{17}$$

Working in the HNC approximation, the description of the colloid–microion correlation turns out to be improved with respect to linearized theories in two aspects. On the one hand we

include the effect of colloid–colloid correlations via the Ornstein–Zernike equations (4). The importance of including this contribution is especially evident when we compare the theoretical colloid–ion distributions with simulation results at finite colloidal density [25]. On the other hand, the use of the HNC closure implies the addition of non-linear terms in the description of the ionic profiles around the colloidal particle [8].

As we will see below, the use of the HNC approximation for the colloid–microion correlations leads to instabilities in certain situations. In order to surmount this drawback we have tested the Zerah–Hansen closure [20] for *attractive* colloid–microion interactions only[2]. Nevertheless, this alternative does not produce in principle physically consistent results. A more detailed discussion of this fact in connection with the non-solution boundary will be given in section 5.

As mentioned, equations (16), (17) are solved for the three colloid–microion TCFs in conjunction with the OZ equations (4). This means that we incorporate into the calculation the effect of microion–microion correlations (via the simple approximation (15)) as well as the colloid–colloid correlations. Due to this latter contribution, a certain colloid–colloid structure should be provided as input to solve the colloid–microion structure. We will see that this can be done self-consistently or, alternatively, we can carry out a single calculation for a particularly simple colloid–colloid distribution function.

Step 6: solution of the effective colloid–colloid problem

Once we have solved the colloid–microion correlation, and obtained the corresponding DCFs, the effective potential between colloids is completely determined via equations (14) and (15). In the OCS, this potential induces a colloid–colloid pair structure that is obtained using the main-force potential

$$w(r) = \beta u'_{\rm eff}(r) - h(r) + C(r) + B_{\rm cc}(r), \tag{18}$$

where $u'_{\rm eff}(r)$ is defined in equation (14) and $B^0_{\rm cc}$ is the colloid–colloid bridge function. In this work we have assumed that $B^0_{\rm cc} = 0$ (HNC approximation). The extension of the theory for large packing fractions of colloids would require introducing hard-sphere bridge functions as has been done elsewhere [25].

General strategy

Both steps 5 and 6 involve the solution of an integral equation for only one type of correlations, keeping the rest fixed. In view of this, we iterate over steps 5 and 6 until self-consistency is achieved. The result should be equivalent to the solution of the full multi-component OZ equations with RPA, and HNC closures for the microion–microion, colloid–microion and colloid–colloid correlations respectively. The result of the calculation will be self-consistent colloid–colloid pair distribution functions and effective potentials. The calculations were done numerically using fast-Fourier transform methods with 4096–16 386 points and a grid interval of 0.01–0.5 nm. The Ng and Broyles strategies [31] were employed to accelerate convergence. Fully converged results can be obtained in a few minutes on a standard PC in most cases. For highly coupled systems it can be needed to start the calculation at a higher temperature or at a lower colloidal charge. These calculations serve as first estimates to perform the calculation at the desired temperature or colloidal charge.

[2] The reason for using the ZH closure for attractive interactions only lies in the fact that we wan to keep the number of fitting parameters as low as possible. As discussed below, the origin of the non-solution instabilities is related to a poor description of the colloid–counterion correlation.

As we will see, full self-consistency cannot be accomplished in certain cases, especially in the low-salt limit and also at low colloidal concentrations and high colloidal charges. This means that the integral equation defined above does not have a solution for these situations. Nevertheless we can obtain a fairly accurate estimation of the effective potential and colloid–microion distributions if we solve the colloid–microion problem (step 5) for a fixed colloid–colloid structure. A convenient choice for this is to use the colloid–colloid $g(r)$ obtained from the solution of the one-component HNC equation for the DLVO effective pair potential. Even if this solution does not correspond to the full self-consistent solution of the CGHNC integral equation it can be helpful to explain the behaviour of these systems.

3. Colloid–colloid correlations and effective potentials

In order to test unambiguously the accuracy of the CGHNC equations and the approximations implicit in them, we need to compare with simulation results for the same colloidal models. To our knowledge, there is just one simulation study of charged colloidal mixtures with added electrolyte in which colloid–colloid pair distribution functions are reported [17]. An analogous system was studied by Angelescu and Linse [18], although their work focused on the computation of the mean-force potential between two charged colloids in the presence of salt. Both works were oriented to elucidate some experimental results which showed the existence of salt-driven reentrant transitions in aqueous mixtures of sodium dodecyl sulfate and $Al(NO)_3$.

In this work we have performed CGHNC calculations for hard-core spherical colloids of charge $Z_c = 60$ in the presence of variable amounts of 1:z_c electrolyte, with z_c being the charge of the electrolyte counterions. The size of the particles is 4 and 0.4 nm for colloids and microions respectively. Following Lobaskin and Qamhieh [17], we have considered three choices for the counterion charge: $z_c = 1, 3, 5$. Results for the colloid–colloid radial distribution function can be found in figures 1 and 2 for the monovalent and the pentavalent cases respectively.

Unfortunately, the full CGHNC integral equation cannot be solved for most of the cases reported by Lobaskin and Qamhieh [17] except at moderate salt concentrations. In the monovalent case the theoretical result is virtually exact, whereas in the pentavalent case the CGHNC overestimates by far the height of the main peak. As we will see in the next two sections, this mismatch and the lack of solutions is due to the proximity of a salt-driven phase separation. In this connection, the use of the Zerah–Hansen closure [20] for the *colloid–counterion* correlation makes it possible to solve the integral equation at lower salt concentrations, although this improvement should be attributed to a crude description of the colloid–counterion correlation near the colloidal surface.

We must note that the CGHNC equation can be solved with reasonable accuracy for charge and size asymmetries beyond the limit of the standard HNC equation. As mentioned in the introduction, this feature was already made evident previously for colloid–counterion mixtures [26]. As regards suspensions with added electrolyte, it has been reported very recently that the full HNC equation cannot be solved for charge asymmetries larger than 450 for 1:1 electrolyte of concentration 0.001 M [32]. By means of the CGHNC procedure we can obtain results for systems with charges up to 800–1200 and salt concentrations of 10^{-1}–10^{-6} M, depending on the system. For the most difficult case studied by Lobaskin and Qamhieh [17] (low colloidal packing fraction and low salinity) the improvement is more modest: for instance for the case studied in figure 1 the full HNC can be solved up to a concentration of 0.075 M. The CGHNC permits extending the calculation limit up to 0.066 M.

Results for the colloid–microion radial distribution functions can be found in figure 3. For the concentrations for which the full CGHNC integral equation cannot be solved we have

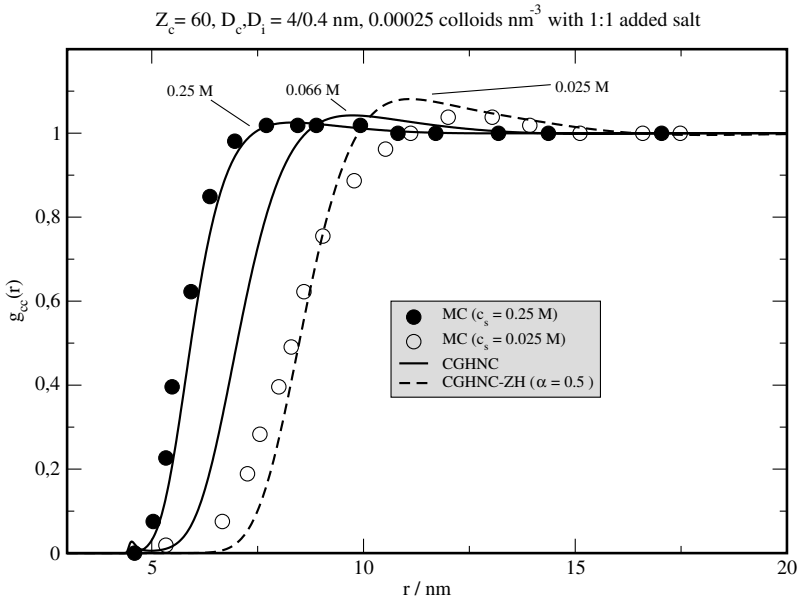

Figure 1. Colloid–colloid radial distribution functions for aqueous suspensions of hard-core colloids of charge 60 electrons in the presence of colloid counterions and variable amounts of 1:1 added salt. The diameter of the colloids and the microions is 4 and 0.4 nm respectively. The Monte Carlo (MC) results were taken from [17]. The solid lines stand for CGHNC predictions. The dashed line corresponds to the use of the ZH closure for colloid–counterion correlation only. See text for details.

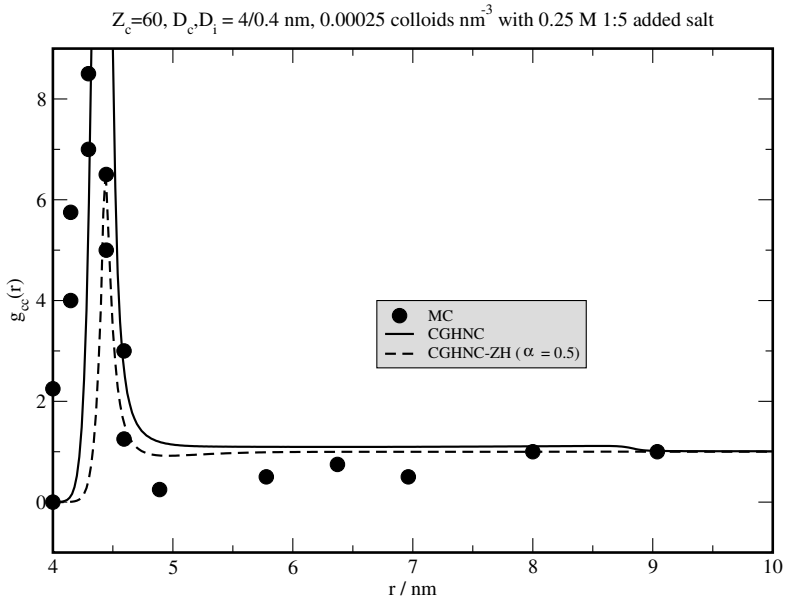

Figure 2. Same as figure 1 but for 1:5 added salt (salt counterions are pentavalent).

plotted the results obtained with the simplified procedure mentioned in section 2. According to this the colloid–counterion part of the theory is solved for a fixed colloid–colloid radial

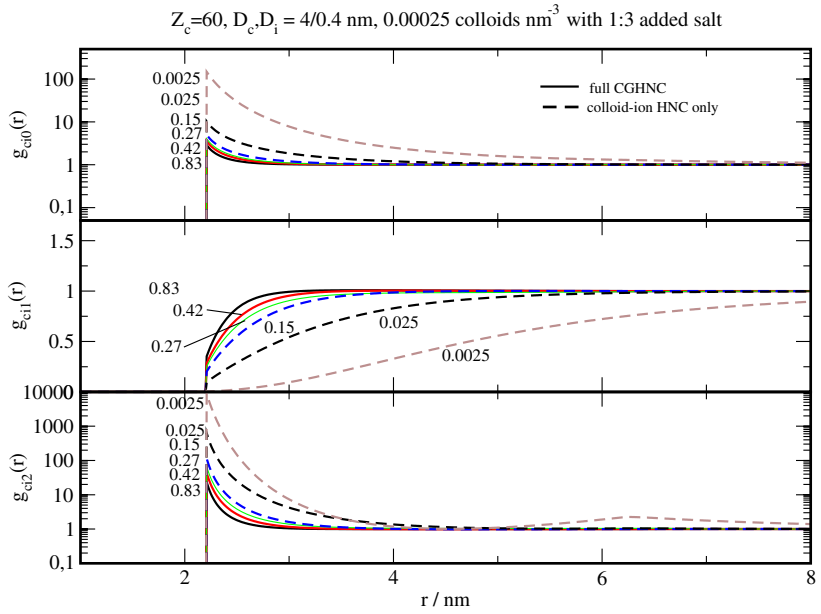

Figure 3. Colloid–monovalent counterion (upper panel), colloid–coion (medium panel) and colloid–trivalent counterion (lower panel) radial distribution functions for hard-core colloidal suspensions in the presence of 1:3 added salt. Solid lines correspond to the full solution of the CGHNC equations, whereas the dashed lines represent a partial solution in which only the colloid–microion structure is solved (see text for details).

distribution function. This is extracted in turn from the solution of the one-component HNC integral equation for the DLVO effective potential at the same salt concentration.

The curves displayed in figure 3 reproduce reasonably well the Monte Carlo (MC) results of [18] for the colloid–counterion correlation. For instance, at a salt concentration of 0.025 M, contact values of 9.3 and 628 are obtained for the colloid–monovalent counterion and colloid–trivalent counterion respectively. The MC estimations are ∼9 and ∼500 respectively, which shows that the HNC closure together with the RPA approximation for microion–microion correlations tends to *overestimate* the accumulation of trivalent ions in the proximity of the colloidal surface. On the other hand the prediction of the colloid–coion correlation is not so accurate. The CGHNC results do not exhibit the same accumulation of coions at intermediate distances that can be clearly observed in the MC curves of [18]. This is a consequence of using a simple approximation for microion–microion correlations within the CGHNC approach. This suggests that a better approximation than RPA would be needed to reproduce the system behaviour correctly.

In order to shed light on the performance of the RPA approximation we have looked at the counterion–counterion radial distribution functions. It must be noted that, in the context of the CGHNC formalism, the ion–ion correlations are not obtained explicitly. However, it is possible to make use of the Ornstein–Zernike relations (4) to extract the counterion–counterion radial distribution function once the full self-consistent solution is found. Results for a 60:z ($z = 1, 2, 3$) hard-core *salt-free* system are presented in figure 4 along with MC data [33]. In this figure it can be observed that the agreement between theory and simulation is fairly qualitative. The mismatch gets worse as we move from monovalent to trivalent counterions. For this latter case the CGHNC function gives a maximum value of

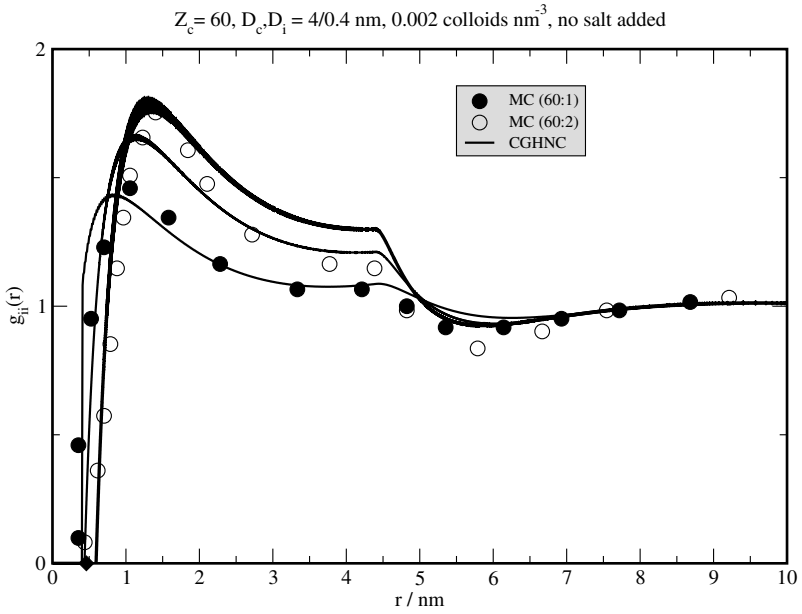

Figure 4. Counterion–counterion radial distribution functions extracted from the CGHNC equations (solid lines) for colloid–counterion hard-core mixtures in the absence of salt. The charge of the colloids is 60 electrons and the counterions have, from top to bottom, charges of 1, 2 and 3 respectively. MC results for the same systems extracted from [33] are also included in the graph.

1.8, whereas the simulation result (outside the graph) is 6.4. These results suggest that the RPA approximation only works well for monovalent counterions. In the multivalent case microion–microion correlations are not captured correctly and this explains why the integral equation fails at situations in which microion–microion correlations play a crucial role, that is, condensation of counterions at the colloidal surface and charge inversion [34]. This fact also accounts for the fact that the non-solution boundaries appear when the Debye length is not short enough to cancel the microion–microion correlations, that is, low colloidal packing fractions and low salt concentrations.

In figure 5 we report results for the colloid–colloid effective potentials which are obtained in the context of the CGHNC formalism. It must be pointed out that the potentials shown in this figure do not represent true effective interactions. They correspond to the function denoted by $u'_{\rm eff}(r)$ in equation (14) and do not include the bridge function contribution. We have seen in our previous paper [26] that the effective potential approximated in this way develops an attractive minimum in the vicinity of the non-solution region. Whether this minimum is spurious or not is difficult to tell. As can be seen in figure 5, the CGHNC 'effective' potential at very low ionic strengths exhibits a very deep minimum at short distances. This is not observed in the MC results of [16], where it was found that the effective potentials are repulsive at all distances for monovalent counterions. In fact the CGHNC 'effective' potential for the salt-free case does not compare very well with the MC effective interaction [16] and it shows Yukawa-like behaviour at long distances only. However, at moderate salt concentrations the minimum of the CGHNC effective potential is located at the same distance (around 4.5 nm) at which it appears in the *mean-force* potentials obtained from MC simulations with added salt for the same system [18]. Due to the artificial enhancement of this minimum as the salt concentration is lowered, effective potentials extracted from this integral equation are not reliable in the

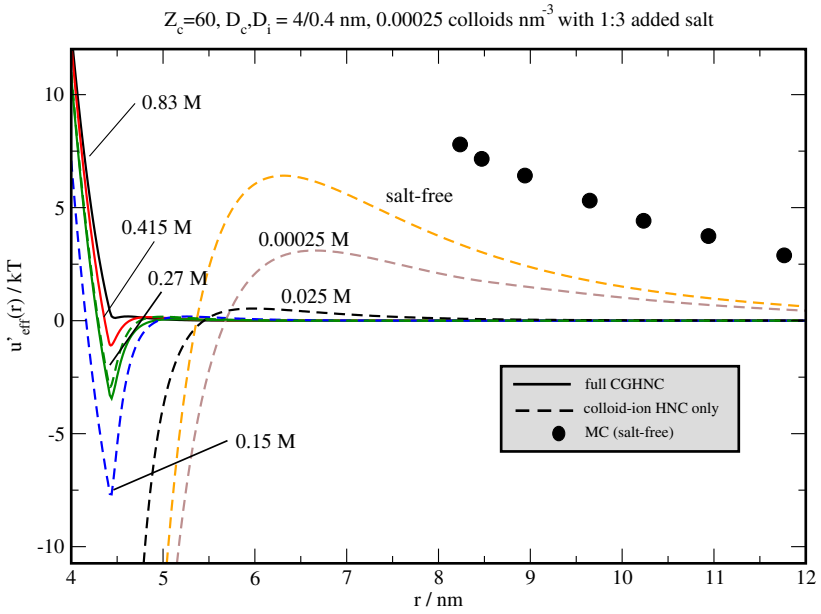

Figure 5. Colloid–colloid effective potentials for hard-core colloidal suspensions in the presence of 1:3 added salt as obtained from the solution of the CGHNC equations. The colloidal and microion parameters are the same as those considered in figures 1 and 2. Solid lines correspond to the full solution of the CGHNC equations whereas the dashed lines represent a partial solution in which only the colloid–microion structure is solved (see text for details). MC results from [16] are also shown in the graph.

vicinity of the non-solution region. This is also common to other integral equation theories unless a good approximation for the bridge functions occurring in equation (14) is provided.

In spite of this drawback, we have also compared the CGHNC effective potentials with experimental measurements for this quantity. In order to do this we have chosen the work by Crocker and Grier [35]. Results for the effective potential at the same conditions studied by these authors are presented in figure 6. It must be noted that in this case there are two unknown parameters that should be included in the description of the experimental data. These are the colloidal charge and the concentration of the background electrolyte which, at highly deionized conditions, cannot be determined with accuracy. Crocker and Grier proposed a background salt concentration of around 10^{-6} M. Playing with this parameter, together with the colloidal charge, we can fit the experimental potential. In figure 5 we can see that the CGHNC fits the experiment for a larger charge than that obtained when using the DLVO potential. Both potentials are essentially identical at long distances but they differ at short distances, the CGHNC potential being less repulsive in this region. We should bear in mind that the DLVO potential arises from a *linearized* solution of the Poisson–Boltzmann equation and this linearization is not accurate near the colloidal surface, especially for large charges. This explains why a lower charge is needed to fit the experimental results with the DLVO potential.

The difference between DLVO and CGHNC becomes more perceptible if we increase the colloidal packing fraction. Crocker and Grier obtained their results in the very dilute regime for which, in deionized conditions, the DLVO theory performs well. However, it is interesting to see how the effective potential becomes increasingly less repulsive as we move towards

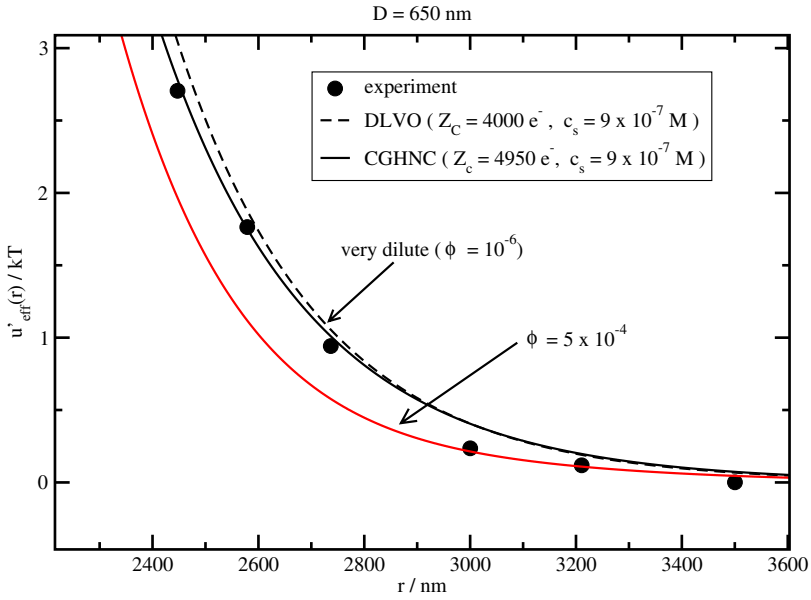

Figure 6. Effective potentials from CGHNC and DLVO theories for the same experimental system considered by Crocker and Grier [35]. Results for two different colloid packing fractions (ϕ) are shown in the figure.

more concentrated systems. This effect has already been observed previously by other authors using a more sophisticated integral equation formalism [20].

4. Salt-driven phase separation

In previous experimental and simulation studies a salt-driven phase separation has been reported for aqueous mixtures of micelles and an electrolyte containing multivalent counterions [17, 18]. According to these studies the suspensions are stable at deionized conditions as well as at very high concentrations of salt. Nevertheless, in the intermediate region the system coagulates.

We have explored this transition using the CGHNC formalism. The system is the same as that described in the previous section (figures 1 and 2) and studied by Lobaskin and Qamhieh [17] and Angelescu and Linse [18]. The results that illustrate the predictions of the theory for this system can be found in figures 5–8. We find that the numerical solution of the integral equation diverges if the added salt concentration is sufficiently low. This feature happens for 1:1, 1:3 and 1:5 electrolytes, although the salt concentration for which the instability appears in the 1:1 case is much lower than in the other cases. This is not the only difference between electrolytes with monovalent and multivalent counterions. If we look at the long-wavelength limit of the colloid–colloid structure factor (figure 7) we observe that the lack of solution of the integral equation is associated to a divergence of this magnitude when we have multivalent counterions. This divergence does not occur in the 1:1 case. This suggests that the suspension phase separates in the presence of multivalent ions only. These results are consistent with the findings of Lobaskin and Qamhieh [17].

These authors explain this phase separation by making use of the charge-reversal concept: at low ionic strengths the effective potential is purely repulsive. When we increase the

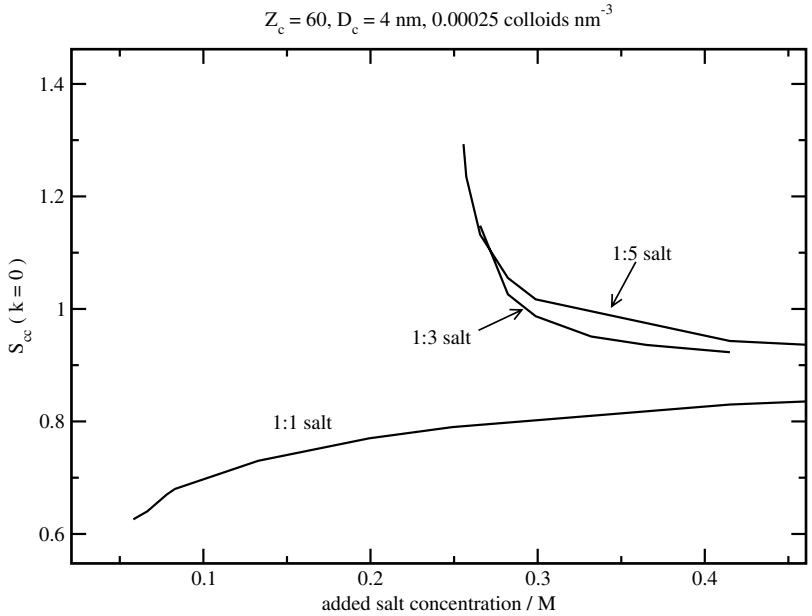

Figure 7. Long-wavelength limit of the CGHNC colloid–colloid structure factor for the same hard-core colloidal suspensions considered in figures 1 and 2.

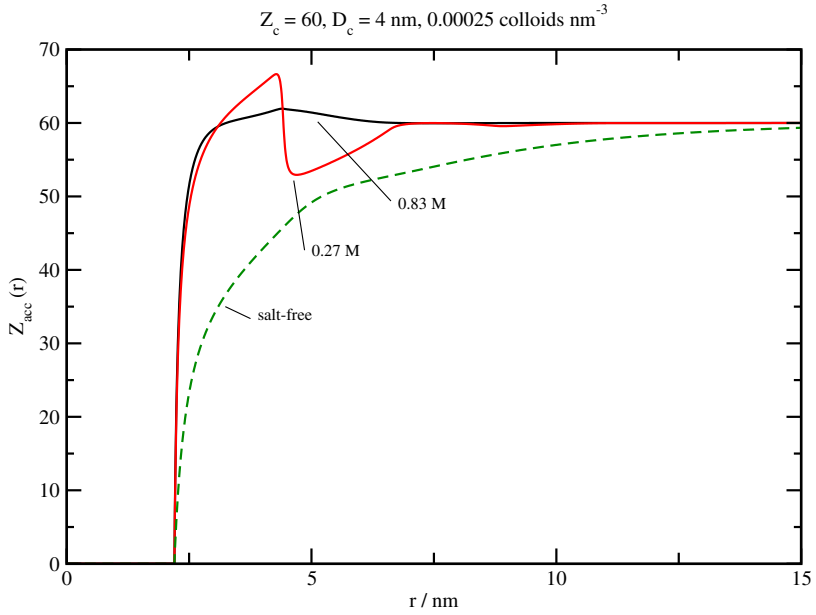

Figure 8. Accumulated running charge around the colloid for the system with 1:3 added salt (same system as considered in figure 3). The solid and dashed lines have the same meaning as in figures 3 and 5.

concentration of salt, counterions accumulate in the vicinity on the colloidal surface and reduce the effective charge. If the amount of salt is high enough, and it is in certain proportion to

the colloidal concentration, the system ceases to be stable and coagulates. Adding more salt makes the effective charge change sign, and this originates an effective interaction which is again basically repulsive, causing the system to redissolve. In order to see if the CGHNC theory is capable of reproducing this charge-reversal effect, we have looked at the colloid–microion radial distribution functions and calculated the total accumulated charge around the colloid as a function of the distance. The results are shown in figure 8. We can see that at low ionic strengths the accumulated charge is monotonic and shows no change of sign. However, at intermediate and large salt concentrations the same function undergoes a rapid increase at short distances. This would indicate that the colloid bears an apparent charge of opposite sign. This is only strictly true at high salt concentrations. At intermediate concentrations the change reversal is partially compensated by an oscillation of the total accumulated charge at around 5 nm. This explains why, in this case, the colloids feel a net attraction which causes the system to coagulate.

At this point it must be stressed that, as already mentioned, the charge-reversal effect is a consequence of microion–microion correlations at the colloidal surface [34] and that these are treated in a very crude manner within the present theory. Although similar approximations like the HNC/MSA are capable of reproducing overcharging in a semiquantitative manner [36], it must be borne in mind that the disagreement between theory and simulation is due principally to a poor description of these correlations.

The 'reentrant' transition can also be intuitively perceived when we look at the 'effective' potentials of figure 5. We see that at high salt concentrations the CGHNC interaction is purely repulsive. This feature makes the suspension stable against coagulation. If we decrease the ionic strength of the system an attractive well appears in the CGHNC effective potential. As already mentioned, this minimum is located at the same distance (around 4.5 nm) as the *mean-force* potentials of Angelescu and Linse [18]. The presence of this minimum at salt concentrations close to the divergence of $S(k)$ (cf figure 7) explain the coagulation of the system at intermediate ionic strengths. If we keep decreasing the salt concentration we find that the CGHNC effective potential develops a repulsive barrier at longer distances. At sufficiently low ionic strength this barrier can have a height of around 2–3 $k_{\mathrm{b}}T$ and this explains why the suspension becomes stable again as we approach the salt-free limit.

Concerning the origin of the attractive features of the effective potential, figure 3 shows that there is a strong accumulation of counterions near the colloidal surface. This accumulation becomes more and more intense as we decrease the concentration of salt. Moreover, the contact values for trivalent counterions are obviously larger than for monovalent ones. In addition the correlation function of the former decays more rapidly than the latter. This fact indicates that the trivalent counterions replace the monovalent ones in the screening of the colloidal charge as we decrease the concentration of salt. The presence of these trivalent counterions in the colloidal screening cloud leads to effective attractions at intermediate salt concentrations due to the interaction between the colloids and the screening clouds of their neighbours. When we move to larger salt concentrations this attraction becomes less important than the repulsion between the clouds themselves. The fact that the attraction, and hence the non-solution boundaries, appear at higher salt concentrations than those observed in the simulation is, again, a consequence of a too simplistic treatment of microion–microion correlations.

5. Discussion and origin of the non-solution regions

In the previous sections we have shown that the CGHNC formalism produces results and conclusions which are consistent with experiments and MC simulations. This suggests that it can be judicious to introduce certain approximations into the Ornstein–Zernike formalism

that take advantage of the asymmetry of the mixture. The idea is to reduce the complexity of the numerical procedure in order to broaden the region of solution. Nevertheless, the integral equation employed here remains unsolvable in many cases of physical interest, as comparison with simulations and experiments demonstrated. The use of an *incomplete* solution (keeping the colloid–colloid correlation fixed) permitted us to obtain at least the colloid–microion structure and approximate effective potentials. But still we can wonder about the reasons why the numerical solution of the integral equation does not converge at certain situations.

We must say that in most cases the non-solution boundaries are associated to the proximity of a phase instability. This statement should be taken with caution because it has been demonstrated that the non-solution line of the HNC integral equation does not have the characteristics of a spinodal [24]. Thus, we cannot use the non-solution properties of the integral equation to locate the precise onset of the phase separation but we can at least predict its existence.

In previous works [25, 26] we discussed the nature of the non-solution boundary of the CGHNC integral equation. We showed that the equation becomes increasingly more difficult to solve the larger is the colloidal charge and the smaller the colloidal size. We also found that in the proximity of a non-solution boundary the effective potential becomes attractive. This feature seems to be connected to a gas–liquid transition. A similar finding is obtained in the context of this work when we monitor the behaviour of the system as we decrease the concentration of salt. This phenomenon can be clearly seen in figure 7, for instance. Nevertheless, as already mentioned, the occurrence of attractions in the effective potential can be spurious.

In figure 9 we can see that as we approach the non-solution boundary of the CGHNC integral equation, the effective potential develops a minimum at short distances. This provokes an instability that makes the equation diverge at lower salt concentrations. As we saw in section 4, this instability seems to correspond to a real phase transition [18] when there are multivalent ions present in the system, as monitoring of the isothermal compressibility (figure 7) reveals.

In section 4 we also saw that the HNC closure tends to overestimate the local concentrations of counterions close to the colloidal surface. Bearing this in mind we have also considered the Zerah–Hansen (ZH) closure [37] for attractive colloid–microion correlations only (see footnote 2). This means that we evaluate the colloid–counterion total correlation function by means of

$$h_{\mathrm{cm}}(r) = \frac{\exp(f(r)[-\beta u_{\mathrm{cm}}(r) + h_{\mathrm{cm}}(r) - C_{\mathrm{cm}}(r)]) - 1}{f(r)} \tag{19}$$

with $f(r) = 1 - \exp(-\alpha r)$ and α being an adjustable parameter. Equation (19) interpolates between the MSA closure at short range and the HNC at long range. As we can see in figure 9, the use of the ZH closure eliminates the minimum in the effective potential and makes the interaction purely repulsive. As a consequence, the ZH closure permits us to obtain a solution at lower salt concentrations (see figure 1). The good performance of the ZH closure in this respect has already been pointed out [20, 38].

We should wonder about the reasons for such a behaviour. As mentioned, the ZH closure for attractive interactions involves using the MSA approximation at short distances and the HNC at longer ones. It is known that the MSA approximation underestimates the colloid–counterion pair distribution function close to contact for highly charged systems [21]. This feature compensates the tendency of the HNC to overestimate this value (see above). Therefore the good behaviour of the ZH closure should be considered as the result of a convenient cancellation of errors and, therefore, not due to clear physical reasons. As a matter of fact, in the context of the CGHNC formalism, it was not possible to fix the α parameter contained

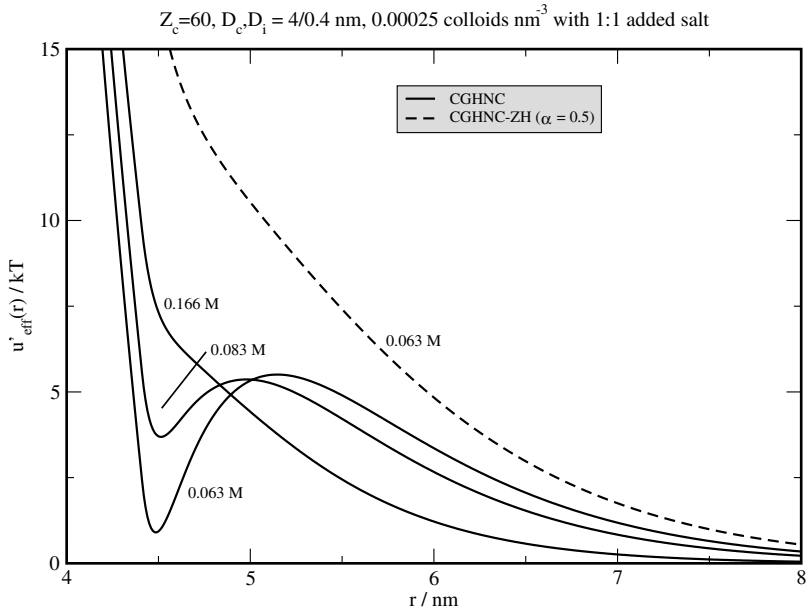

Figure 9. Effective potentials at different salt concentrations for the same system considered in figure 1. The solid lines corresponds to CGHNC results obtained using the HNC closure for all colloid–microion correlations whereas the dashed line stands for the use of the ZH closure for colloid–counterion correlations only (see text for details).

in function $f(r)$ in equation (19) by requiring thermodynamic consistency. In contrast, a more sophisticated approach in which all correlations are treated in the ZH approximation [20] permits us indeed to optimize all the αs using several optimization criteria. This means that we need a very cumbersome integral equation to obtain accurate results in these systems. A simplified procedure like the CGHNC can be helpful only if we use α as an empirical fitting parameter.

In any case, a general feature of the present theory is its failure when the Debye screening constant becomes too low (low colloidal packing fractions and/or low salinities). As already mentioned, this is a consequence of the poor description of the microion–microion correlations, which become important when the electrostatic coupling is very large. Thus the theory turns out to be imprecise or unsolvable when phenomena like overcharging and like-charge attraction appear in the system.

6. Conclusions

In this paper we have extended the CGHNC theory to charged colloidal suspensions with added salt. This implies introducing the following approximations in the solution of the multicomponent Ornstein–Zernike equation.

(1) All microion–microion correlations are evaluated in the RPA approximation and considered independent from colloid–colloid and colloid–microion correlations.
(2) Colloid–microion correlations are evaluated in the HNC approximation (colloid–microion bridge functions ignored).

(3) Colloid–colloid correlations are solved in the HNC approximation for an effective pair potential which is obtained assuming that colloid–colloid bridge functions are negligible.
(4) Additionally the colloid–microion HNC integral equation can be solved for a fixed colloid–colloid structure. This can be extracted from the solution of the one-component HNC equation for the DLVO effective potential.

The success of this integral equation procedure is limited. The solution region is extended but at the price of losing accuracy in the prediction of the colloid–colloid and colloid–microion radial distribution functions, especially for multivalent microions. The effective potential also exhibits a spurious minimum when the non-solution region is approached. This feature is related to strong accumulation of counterions in the vicinity of the colloid surface (which causes the ionic 'atmospheres' to attract each other) and poor description of microion–microion correlations. This drawback can be surmounted if we use the ZH closure for attractive colloid–microion correlations only, although this requires introducing an adjustable parameter.

In spite of this limited performance, the results obtained here provide a semi-quantitative description of the colloidal system and a means to elucidate the occurrence of salt-driven transition suspensions with multivalent added salt. The CGHNC results reveal divergences of the long-wavelength limit of the colloid–colloid structure factor and charge reversal connected to the appearance of attractive minima in the effective potential.

The results obtained here show also that a more precise description of the system requires a better evaluation of the microion–microion correlations, especially for multivalent microions, and the introduction of suitable bridge functions. The 'coarse-graining' approximation implicit to the CGHNC procedure should be used with caution in these strongly interacting systems.

Acknowledgments

We thank Dr F Bresme for discussions and a critical reading of the manuscript. This work has been supported by the Spanish *Dirección General de Investigación Científica y Técnica* under grants BQU2001-3615-C02-01 and VEM2003 20574 C03 01.

References

[1] Evans D F and Wennerström H 1999 *The Colloidal Domain, where Physics, Chemistry, Biology and Technlogy Meet* (New York: Wiley–VCH)
Russel W B, Saville D A and Schowalter W R 1989 *Colloidal Dispersions* (Cambridge: Cambridge University Press)
[2] Frenkel D 2000 Introduction to colloidal systems *Proc. 53rd Scottish Universities Summer School in Physics* ed M E Cates and M R Evans
[3] Hansen J P and McDonald I R 1990 *Theory of Simple Liquids* 2nd edn (New York: Academic)
[4] Derjaguin B V and Landau L D 1941 *Acta Physicoquim. URSS* **14** 633
Verwey E J W and Overbeek J Th G 1948 *Theory of the Stability of Lyophobic Colloids* (Amsterdam: Elsevier)
[5] van Roij R, Dijkstra M and Hansen J-P 1999 *Phys. Rev.* E **59** 2010
[6] Chan D Y C 2001 *Phys. Rev.* E **63** 061806
[7] Denton A R 2000 *Phys. Rev.* E **62** 3855
[8] Denton A R 2004 *Phys. Rev.* E **70** 031404
[9] Tamashiro M N and Schiessel H 2003 *J. Chem. Phys.* **119** 1855
[10] von Grünberg H H, van Roij R and Klein G 2001 *Europhys. Lett.* **55** 580
[11] Forsman J 2004 *J. Phys. Chem.* B **108** 9236
[12] Trizac E and Levin Y 2004 *Phys. Rev.* E **69** 031403
[13] Stevens M J, Falk M L and Robbins M O 1996 *J. Chem. Phys.* **104** 5209
[14] Lobaskin V and Linse P 1998 *J. Chem. Phys.* **109** 3530
[15] Messina R, Holm C and Kremer K 2000 *Phys. Rev. Lett.* **85** 872

[16] Lobaskin V, Lyubartsev A and Linse P 2001 *Phys. Rev.* E **63** 020401
[17] Lobaskin V and Qamhieh K 2003 *J. Phys. Chem.* B **107** 8022
[18] Angelescu D G and Linse P 2003 *Langmuir* **19** 9661
[19] Caccamo C 1996 Integral equation theory description of phase equilibria in classical fluids *Phys. Rep.* **274** 1–106
[20] González-Mozuelos P and Carbajal-Tinoco M D 1998 *J. Chem. Phys.* **109** 11074
Carbajal-Tinoco M D and González-Mozuelos P 2002 *J. Chem. Phys.* **117** 2344
[21] Belloni L 1986 *J. Chem. Phys.* **85** 519
[22] Belloni L 2000 *J. Phys.: Condens. Matter* **12** R549
[23] Belloni L 1986 *Phys. Rev. Lett.* **57** 2026
[24] Belloni L 1993 *J. Chem. Phys.* **98** 8080
[25] Anta J A and Lago S 2002 *J. Chem. Phys.* **116** 10514
[26] Anta J A, Bresme F and Lago S 2003 *J. Phys.: Condens. Matter* **15** S3491
[27] Ashcroft N W and Langreth D C 1967 *Phys. Rev.* **156** 685
[28] Anta J A and Louis A A 2000 *Phys. Rev.* B **61** 11400
[29] Xu H and Hansen J P 1998 *Phys. Rev.* B **57** 211
[30] Henderson R L 1974 *Phys. Lett.* A **49** 197
[31] Ng K 1974 *J. Chem. Phys.* **61** 2680
Broyles A A 1960 *J. Chem. Phys.* **33** 2680
[32] Leger D and Levesque D 2004 *Preprint* cond-mat/0412086 v2
[33] Lobaskin V and Linse P 2000 *J. Mol. Liq.* **84** 131
Linse P and Lobaskin V 2000 *J. Chem. Phys.* **112** 3917
[34] Grosberg A Y, Nguyen T T and Shklovskii B I 2002 *Rev. Mod. Phys.* **74** 329
[35] Crocker J C and Grier D G 1996 *Phys. Rev. Lett.* **77** 1897
[36] Desserno M, Jiménez-Ángeles F, Holm C and Lozada-Cassou M 2001 *J. Chem. Phys.* **105** 10983
[37] Zerah G and Hansen J P 1986 *Phys. Rev. Lett.* **79** 3082
[38] Belloni L 1988 *J. Chem. Phys.* **88** 5143